

Accepted Manuscript

Competitive sorption affinity of sulfonamides and chloramphenicol antibiotics toward functionalized biochar for water and wastewater treatment

Mohammad Boshir Ahmed, John L. Zhou, Huu Hao Ngo, Wenshan Guo, Md. Abu Hasan Johir, Dalel Belhaj

PII: S0960-8524(17)30532-1

DOI: <http://dx.doi.org/10.1016/j.biortech.2017.04.042>

Reference: BITE 17937

To appear in: *Bioresource Technology*

Received Date: 17 March 2017

Revised Date: 10 April 2017

Accepted Date: 11 April 2017

Please cite this article as: Ahmed, M.B., Zhou, J.L., Ngo, H.H., Guo, W., Johir, d.A.H., Belhaj, D., Competitive sorption affinity of sulfonamides and chloramphenicol antibiotics toward functionalized biochar for water and wastewater treatment, *Bioresource Technology* (2017), doi: <http://dx.doi.org/10.1016/j.biortech.2017.04.042>

This is a PDF file of an unedited manuscript that has been accepted for publication. As a service to our customers we are providing this early version of the manuscript. The manuscript will undergo copyediting, typesetting, and review of the resulting proof before it is published in its final form. Please note that during the production process errors may be discovered which could affect the content, and all legal disclaimers that apply to the journal pertain.



1 **Competitive sorption affinity of sulfonamides and chloramphenicol**
2 **antibiotics toward functionalized biochar for water and wastewater**
3 **treatment**

4

5 Mohammad Boshir Ahmed¹, John L. Zhou^{1*}, Huu Hao Ngo¹, Wenshan Guo¹, Md. Abu Hasan
6 Johir¹, Dalel Belhaj²

7

8 ¹School of Civil and Environmental Engineering, University of Technology Sydney, Broadway,
9 NSW 2007, Australia

10

11 ²ENIS, Engineering Laboratory of Environment and Eco-technology, LR16ES19, University of
12 Sfax, Sfax, Tunisia

13

14

15

16

17 *Corresponding author

18 Prof John L Zhou

19 School of Civil and Environmental Engineering

20 University of Technology Sydney

21 15 Broadway, NSW 2007

22 Australia

23 Email: junliang.zhou@uts.edu.au

24 **Abstract**

25 Competitive sorption of sulfamethazine (SMT), sulfamethoxazole (SMX), sulfathiazole (STZ)
26 and chloramphenicol (CP) toward functionalized biochar (fBC) was highly pH dependent with
27 maximum sorption at pH ~4.0-4.25. Equilibrium data were well represented by the Langmuir and
28 Freundlich models in the order STZ > SMX > CP > SMT. Kinetics data were slightly better fitted
29 by the pseudo second-order model than pseudo first-order and intra-particle-diffusion models.
30 Maximum sorptive interactions occurred at pH 4.0-4.25 through H-bonds formations for neutral
31 sulfonamides species and through negative charge assisted H-bond (CAHB) formation for CP, in
32 addition to π - π electron-donor-acceptor (EDA) interactions. EDA was the main mechanism for
33 the sorption of positive sulfonamides species and CP at pH < 2.0. Sorption of negative
34 sulfonamides species and CP at pH > 7.0 was regulated by H-bond formation and proton
35 exchange with water by forming CAHB, respectively. The results suggested fBC to be highly
36 efficient in removing antibiotics mixture.

37

38 *Keywords:* Sorption; Sulphonamides; fBC; Electron-donor-acceptor; CAHB

39

40 1. Introduction

41 The use of different antibiotics resulted in reduction of the mortality and morbidity rates from
42 epidemic and infectious diseases such as syphilis, tuberculosis, pneumonia, gonorrhoea, and
43 communicable diseases of childhood (Carvalho and Santos, 2016; Cui et al., 2016; Rajapaksha et
44 al., 2014). The occurrence of antibiotic residues in the environment is attracting attention due to
45 their potential long-term adverse effects on human and animals (Ahmed et al., 2015; Ahmed et
46 al., 2017a; Zhao et al., 2016; Wang et al., 2017). In addition, antibiotics are of great concern as
47 they are consumed in significant quantities all over the world and can particularly act on
48 microorganisms without affecting cells and tissues (Ahmed et al., 2017a; Seifrtová et al., 2009).

49 Physical treatment processes have been found very effective and economic in removing
50 antibiotics among which sorption has emerged as a cost effective method for pollutant removal;
51 unaffected by the potential toxicity as for biological processes; and easy to design and operate
52 (Ahmed et al., 2017a; Yu et al., 2016; Xie et al., 2016). In addition, sorption is an extremely
53 important process because it may dramatically affect the fate and impacts of contaminants in the
54 environment through different mechanisms (Maskaouri and Zhou, 2010). The efficiency of
55 sorption process is highly affected by the properties of sorbate, sorbent, and operating conditions
56 (Azhar et al., 2016). The degree of sorption mainly depends on the physicochemical properties of
57 the micropollutants, type of solid matrices, surface area, porosity, pore diameter, and
58 environmental conditions (Pavlović et al., 2014; Veksha et al., 2014; Yu et al., 2016).

59 The sorption of antibiotics onto carbonaceous materials such as biochar (Yu et al., 2016;
60 Ahmed et al., 2016a; Ahmed et al., 2017b; Yao et al., 2012), activated carbon (Grover et al.,
61 2011), carbon nanotubes (Ahmed et al., 2015), graphene, clay minerals (Ahmed et al., 2015), and
62 hollow polymer nanorods (Xie et al., 2016) has been widely studied and proved very effective
63 (Ahmed et al., 2015). The sorption of antibiotics using biochar was found particularly efficient

64 (Ahmed et al., 2015; Ahmed et al., 2016b). Biochar has a high hydrophobicity and aromaticity
65 and is an excellent sorbent for hydrophobic organic contaminants e.g. aromatics (Lian et al.,
66 2014; Wang et al., 2016). To date, the majority of adsorption studies on the removal of different
67 antibiotic residues by carbonaceous sorbents have been conducted using single solutes, and only
68 a few studies were reported based on the competitive nature of micropollutants (Ahmed et al.,
69 2017b; Calisto et al., 2017; Nielsen and Bandosz, 2016). In addition, the removal mechanisms of
70 antibiotic mixture using different adsorbents are unclear. In reality, aquatic environment can be
71 highly complex including mixtures of different organic and inorganic contaminants, and thus
72 understanding the mechanisms of competitive adsorption is of great importance. During the
73 application of sorbent, sorbate molecules can interact with the same sites of the sorbent particles,
74 hence faster sorption mainly occurs for the compounds which have specific affinity to be sorbed
75 onto the specific surface of sorbent. Interactions are very simple for single solute but can be very
76 complex for a mixture of contaminants. Therefore, we have targeted four antibiotics for their
77 sorption onto functionalized biochar (fBC) in order to check their competitive sorption affinity
78 and to assess the sorption mechanisms as well as sorption trend in different water types.

79 This study aims to bridge the knowledge gap by studying the competitive sorptive
80 capacity and mechanisms by fBC for four widely used antibiotics SMT, SMX, STZ and CP from
81 water and wastewater. Specifically we studied: (i) the effect of pH on competitive sorption with
82 detailed sorption affinity mechanisms, (ii) the kinetics parameters for competitive solutes, (iii) the
83 competitive sorption isotherms parameters, and (iv) the application of fBC in removing
84 antibiotics mixtures from lake water and synthetic wastewater under practical conditions.

85

86 **2. Materials and methods**

87 *2.1. Chemicals and reagents*

88 The antibiotic standards of SMT, SMX STZ and CP were purchased from Sigma-Aldrich,
89 Australia. HPLC-grade organic solvents such as acetonitrile and formic acid were also purchased
90 from Sigma-Aldrich, Australia. Ortho phosphoric acid (85%), hydrochloric acid (35%), sodium
91 hydroxide, potassium chloride, sodium chloride were obtained from Sigma-Aldrich. *Eucalyptus*
92 *globulus* wood was donated by New Forest Asset Management Pty Ltd, Portland, Victoria,
93 Australia.

94

95 *2.2 Preparation and characterization of fBC*

96 fBC was prepared according to Ahmed et al. (2017b). Briefly, 25 g of eucalyptus wood biomass
97 was pyrolyzed at 400 °C at an average heating rate of ~11.0 °C min⁻¹ under constant nitrogen
98 pressure of 2 psi for 2 h, to obtain biochar samples. Biochar functionalization was carried out by
99 soaking 10 g of biochar in 20 mL of 50% ortho-phosphoric acid (oH₃PO₄) for 3 h at 50 °C. The
100 mixture was then reheated at 600 °C for 2 h. After that, the prepared material was left to cool
101 inside the reactor, washed and the pH adjusted to ~7.0, followed by drying overnight at 105 °C,
102 to obtain fBC. The physicochemical characteristics of fBC were extensively examined using
103 Fourier transform infrared spectroscopy (FTIR), Raman spectroscopy, energy dispersive
104 spectrometry (EDS), and zeta potential instrument. The elemental composition of fBC was
105 measured using EDS (Zeiss Evo-SEM). The identification of surface functional groups was
106 conducted using FTIR (Miracle-10, Shimadzu), by measuring the absorbance from 400 to 4000
107 cm⁻¹ using a combined 40 scans. Raman shifts measurement was carried out using Renishaw
108 inVia Raman spectrometer (Gloucestershire, UK) equipped with a 17 mW Renishaw Helium-
109 Neon Laser 633 nm and CCD array detector. Zeta potential values were measured using 500 mg
110 L⁻¹ of fBC dosage at different pH values, after pre-equilibration for 48 h, on Nano-ZS Zeta-seizer

111 (Malvern, Model ZEN3600). Zeta potential was measured three times at each pH (50 scans each
112 time), with the average and standard deviation being calculated.

113

114 *2.3. Competitive sorption experiments using fBC*

115 The stock solutions (100 mg L^{-1}) of SMX, SMT, STZ and CP were diluted to different initial
116 concentrations of each antibiotic. The effects of pH were studied at adjusting pH values from 1.5
117 to 10.9, using HCl and NaOH solutions. fBC was pre-equilibrated at the same pH for 24 h using
118 half of the volume of a mixture of antibiotics and rest of solute was added and shaken for another
119 42 h. The kinetics studies were carried at a pH 4.0-4.25 (where maximum interactions occurred
120 based on pH study) at $25 \text{ }^{\circ}\text{C}$ over 33 h using 80 mg L^{-1} of fBC. Batch competitive experiments
121 were conducted at $25 \text{ }^{\circ}\text{C}$ using 80 mg L^{-1} of fBC with initial concentrations of $0.250\text{-}20.0 \text{ mg L}^{-1}$
122 for each antibiotic in mixture mode which were shaken on an orbital shaker at 120 rpm for 42 h
123 (apparent equilibrium time) at pH 4.0-4.25. In all cases, a constant ionic strength was maintained
124 using 0.01 M NaCl . The control experiments without adsorbents were also executed. The
125 application of fBC to treat lake water (TOC, 96.67 mg L^{-1}) and synthetic wastewater (TOC, 54.0
126 mg L^{-1}) was carried out by spiking each antibiotic (1.0 mg L^{-1}) at pH $\sim 4.0\text{-}4.15$ and $25 \text{ }^{\circ}\text{C}$. TOC
127 was measured by using a TOC analyzer by the filtration of the collected and prepared sample
128 using 1.0 mm pore size syringe filter. Synthetic wastewater was composed of peptone, beef
129 extract, humic acid, tannic acid, arabic acid, sodium lignin sulphonate, acacia gum powder,
130 KH_2PO_4 and $\text{MgSO}_4 \cdot 3\text{H}_2\text{O}$. Control experiments in the absence fBC with different water
131 matrices showed that there was no loss of antibiotics. At equilibrium, the solution pH was
132 measured before the supernatant was taken and filtered through a $0.20 \text{ }\mu\text{m}$ PTFE filter for
133 antibiotic analysis using HPLC.

134

135 2.4. Antibiotics determination and data fitting

136 The concentrations of antibiotics were measured by HPLC (Jasco) equipped with an auto-sampler
 137 and a UV detector at 285 nm, by using 70 μL injection. A reverse phase Zorbax Bonus RP C_{18}
 138 column (5.0 μm , 2.1 \times 1.50 mm, Agilent Technologies) was used for the separation. Mobile
 139 phase A was composed of acetonitrile and formic acid (99.9: 0.1) while mobile phase B was
 140 composed of Milli-Q water and formic acid (99.9: 0.1). The elution started with 15% of A and
 141 85% of B at a flow rate of 0.4 mL min^{-1} , which was changed to 0.3 mL min^{-1} at 0.1 min and
 142 maintained till 5.9 min. Then at 6.0 min the elution changed to 40% of A and 60% of B at a flow
 143 rate of 0.3 mL min^{-1} and maintained over 15 min. The competitive sorption data for all antibiotics
 144 were fitted to the Langmuir and Freundlich isotherm models and three kinetic equations. The
 145 competitive sorption distribution coefficient (K_d , L kg^{-1}) is defined by equation 1:

$$146 \quad K_d = 1000 * \frac{q_s}{C_w} = 1000 * \left(\frac{C_o - C_w}{C_w} \right) \frac{V}{M} \quad (1)$$

147 where q_s is the equilibrium concentration of each antibiotic in mixture mode in sorbent (mg g^{-1}),
 148 C_w and C_o are the equilibrium and initial concentrations (mg L^{-1}) of each antibiotic in mixture
 149 mode, V is the solution volume (L), and M is the sorbent mass (g).

150 The kinetic equations such as the pseudo first order (PFO), pseudo second order model
 151 (PSO) and intra-particle diffusion model (IDM) can be represented as follows:

$$152 \quad \text{PFO: } q_t = q_s(1 - e^{-K_1 t}) \quad (2)$$

$$153 \quad \text{PSO: } q_t = \frac{K_2 q_s^2 t}{1 + K_2 q_s t} \quad (3)$$

$$154 \quad \text{IDM: } q_t = K_i t^{\frac{1}{2}} + C \quad (4)$$

155 Parameters were estimated by nonlinear regression analysis weighted by the dependent variable.

156 Where K_i is the apparent diffusion rate constant ($\text{mg g}^{-1} \text{min}^{-1/2}$), K_1 (min^{-1}) and K_2 ($\text{g mg}^{-1} \text{min}^{-1}$)

157 are PFO and PSO kinetic rate constant, respectively, and C is a constant (mg g^{-1}) that provides
 158 the thickness of the boundary layer.

159 The Langmuir and Freundlich isotherm models can be represented as follows:

160 Freundlich model: $q_s = K_F C_w^{1/n}$ (5)

161 Langmuir model: $q_s = \frac{q_{max} K_L C_w}{1 + K_L C_w}$ (6)

162 where q_{max} is the maximum adsorption capacity (mg g^{-1}), n is a dimensionless number related to
 163 surface heterogeneity, K_F is the Freundlich affinity coefficient ($\text{mg}^{1-n} \text{L}^n \text{g}^{-1}$) and K_L is the
 164 Langmuir fitting parameter (L mg^{-1}).

165

166 3. Results and discussion

167 3.1. Influence of pH on antibiotic K_d during competitive interaction with fBC

168 The K_d values for competitive interaction of selected antibiotics on fBC were found to be pH
 169 dependence (**Fig. 1a**). All the selected sulfonamide antibiotics are ionisable while CP is nonionic.
 170 Lower K_d values were found for all positive sulfonamides species (pH 0-2.0) (Fukahori et al.,
 171 2011; Pei et al., 2014; Teixidó et al., 2011) and CP at pH ~1.50 (2.0×10^4 to $4.5 \times 10^4 \text{ L kg}^{-1}$ for
 172 SMT to STZ). The surface zeta potential value of fBC was found to be pH 2.2 (**Fig. 2**). When pH
 173 was below 2.2, zeta potential value of fBC was found to be positive. Moreover, all sulfonamides
 174 were positively charged at pH < 2.0 (due to matched pK_{a1} values). Thus, lower K_d values were
 175 highly expected due to the repulsion nature of same species and antibiotics might also get
 176 protonated at very low pH. The adsorption of antibiotics at lower pH may be dominated by the
 177 interaction between the protonated aniline ring of antibiotics and the π -electron rich fBC surface
 178 (Zheng et al., 2013).

179 The maximum K_d values were observed at pH ~4.0-4.25 for STZ ($2.2 \times 10^5 \text{ L kg}^{-1}$), SMX
 180 ($1.9 \times 10^5 \text{ L kg}^{-1}$), SMT ($1.7 \times 10^5 \text{ L kg}^{-1}$) and CP ($1.73 \times 10^5 \text{ L kg}^{-1}$). The maximum K_d at this pH

181 range was found due to the adsorption of neutral species of sulfonamides at pH ~2.0-6.0
182 (Fukahori et al., 2011; Pei et al., 2014; Teixidó et al., 2011) and nonionizable CP. The adsorption
183 was due to the formation of strong hydrogen bonds for sulfonamides antibiotics, and due to
184 CAHB for CP.

185 Further increase in pH from 4.5 to higher pH decreased the sorption. However, another small
186 sharp increase of K_d values for all antibiotics was observed at pH ~8.5. The observed K_d values
187 were 5.9×10^4 , 2.6×10^4 , 2.7×10^4 , and 1.8×10^4 L kg⁻¹ respectively for STZ, SMX, SMT and CP.
188 The main reason might be due to sorption of negative species sulfonamides at pH ~6.0-11
189 (Fukahori et al., 2011; Pei et al., 2014; Teixidó et al., 2011) as well as CP declined due to
190 negative surface zeta potential value of fBC leading to electrostatic repulsion. However, the
191 sorption affinity might be due to the formation of CAHB along with EDA interactions (Xie et al.,
192 2014). This was due to the matching of pK_{a2} values of negative species of sulfonamides and
193 surface hydroxyl pK_a values. After that, an increase of pH up to ~11, the sorption was decreased
194 due to highly repulsion nature of negative surface hydroxyl groups and negative species of
195 sulfonamides. The detailed mechanisms were discussed in **section 3.4**.

196

197 3.2. Sorption kinetics in competitive mode

198 Kinetic experiments were carried out for 33 h with the equilibrium being reached within ~1800
199 min. The kinetics of mixture of antibiotics sorption by fBC was fitted to pseudo-first-order
200 (PFO), pseudo-second-order (PSO) and intra-particle diffusion (IPD) models. Based on the
201 correlation coefficient (R^2) and $q_{s,cal}$ (mg g⁻¹) values, the kinetics data for all competitive solutes
202 were slightly better fitted to the PSO chemisorption kinetic model than PFO and IDM models but
203 their R^2 values were comparable (**Fig. 1b**). Based on the $q_{s,cal}$ values in PSO model, antibiotics
204 followed the order of STZ (13.3 mg g⁻¹) > SMX (12.2 mg g⁻¹) > CP (12.3 mg g⁻¹) > SMT (10.9

205 mg g⁻¹). However, the $q_{s,cal}$ values for the PFO kinetic model followed a different order: STZ
206 (10.73 mg g⁻¹) > CP (10.03 mg g⁻¹) > SMX (9.89 mg g⁻¹) > SMT (8.73 mg g⁻¹). IDM and PFO
207 showed slightly lower R^2 values than the PSO model. The IPD rate constant K_i (mg g⁻¹ min^{-0.5})
208 also followed the same trend as the PSO kinetic model $q_{s,cal}$ values.

209

210 3.3. Sorption isotherm models for competitive sorption

211 Compared with the Freundlich isotherm model, interactions of antibiotics with fBC in
212 competitive mode were better fitted to the Langmuir model with higher R^2 values for STZ and
213 SMX. While the Freundlich isotherm model provided a better fit for SMT and CP (**Fig. 3, Table**
214 **1**). The Langmuir sorption capacity (q_{max}) was found to be 45.2, 28.29, 21.35 and 20.71 mg g⁻¹
215 for STZ, SMX, CP and SMT, respectively in competitive mode. The K_F values were 16.76, 9,
216 11.04, 9.81 and 9.65 mg¹⁻ⁿ Lⁿ g⁻¹, respectively, for STZ, SMX, CP and SMT at 25 °C. These
217 findings aligned with the results observed from pH effect and kinetics experiments. Thus, from
218 both models, the sorption affinity can be written in the following order as STZ > SMX > CP >
219 SMT. It is assumed that all the antibiotics in competitive mode share the same sorption sites of
220 fBC when sorbed onto its surface. However, their sorption affinity depends on the
221 physicochemical properties of antibiotics and fBC. The total fBC sorption capacities for all
222 antibiotics in mixture mode were calculated by summarizing individual contributions for both
223 Langmuir model (115.54 mg g⁻¹) and Freundlich model (47.3 mg¹⁻ⁿ Lⁿ g⁻¹). Similar result has
224 been reported for single and competitive sorption of three sulfonamide antibiotics (Ahmed et al.,
225 2017b). Hence, fBC is capable of adsorbing a mixture of antibiotics onto its surface.

226

227 3.4. Mechanisms of competitive sorption on fBC

228 The results from the sorption isotherms, sorption kinetics and the pH effect suggested that the
229 fBC had very strong sorption affinity for antibiotics in competitive mode, while the affinity of the
230 antibiotics sorption onto fBC varied from compound to compound. The sorption of SMT and CP
231 followed the Freundlich isotherm which was related to the chemisorption mechanism. While the
232 sorption of STZ and SMX followed the Langmuir isotherm model related the homogeneous
233 covering of the fBC surface. The kinetic results indicated the sorption of antibiotics in
234 competitive mode agreed well with PSO, PFO and IPD model. This result indicated that the role
235 of surface functional groups, monolayer coverage and diffusion of sorbate molecules during
236 competitive sorption antibiotics. Thus, high competitive sorption affinities of fBC toward
237 antibiotics were due to a combination of effects such as surface homogeneous and heterogeneous
238 sorption sites.

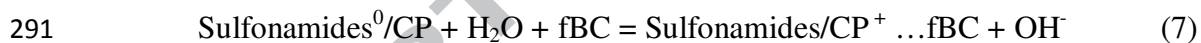
239 All the peaks from the FTIR spectra indicated that fBC contained phenolic -OH , C=O
240 (carboxylic and ketonic), N=C=O (isocyanate), $\text{C}\equiv\text{C}$, and C=C groups on the surface (Ahmed at
241 al., 2016a; Davi and Saroha, 2014; Chen et al., 2016; Tang et al., 2015). FTIR spectra before and
242 after antibiotics sorption clearly show the sorptive nature of fBC. Spectra at $\sim 1516\text{ cm}^{-1}$ (aromatic
243 C=C), at $\sim 2090\text{-}2218\text{ cm}^{-1}$ ($\text{C}\equiv\text{C}$), at $\sim 2276\text{ cm}^{-1}$ (N=C=O), at $\sim 1710\text{ cm}^{-1}$ (C=O , ketonic and
244 carboxylic), at $3620\text{-}3860\text{ cm}^{-1}$ (phenolic, -OH groups), and at $\sim 3020\text{ cm}^{-1}$ (-CH stretch) shifted to
245 lower absorbance areas indicated that antibiotics sorption had been increased by these functional
246 groups on fBC surface. Raman spectra also confirmed this result. In Raman spectra, the D band
247 indicates the degree of disordered SP^2 hybridization of carbon atom containing vacancies,
248 impurities or defects whereas G band indicates the SP^2 hybridization of carbon atoms in any
249 carbonaceous materials (graphitic carbon). The intensity of the peaks was reduced significantly
250 after sorption of antibiotics. The I_D/I_G ratio also decreased which also confirmed the interactions
251 of antibiotics with the surface functional groups of fBC. The peak intensity decreased due to

252 sorption of antibiotics by the fBC functional groups leading to blocking the functional groups
253 available for detecting in Raman spectroscopy. This result also confirmed the role of surface
254 disordered structure carbon atoms i.e. D bands at $\sim 1330\text{ cm}^{-1}$ (in the form of oxygenated
255 functional group) while graphitic G-bands at $\sim 1586\text{ cm}^{-1}$ also decreased indicating the role of
256 C=C i.e. π structured carbon atoms. The latter case can be explained by the electron-donor
257 interaction nature of the arene unit in the C=C and C \equiv C system. Thus Raman spectra indicated
258 the role of functional groups as well as π - π interactions due to change in the peak intensity for G
259 and D bands. In addition, G* band peak intensity also reduced significantly indicating the π - π
260 interactions. The mechanisms of antibiotic sorption can be also explained based on different pH
261 described below.

262 The zeta potential value of the fBC was found to be positive at solution pH 1.5 i.e. surface
263 of the fBC gets protonated. Hence, the weak interactions between the opposite charged
264 quadruples might be the main reason for lower sorption of these antibiotics. However, still there
265 was some sorption which can mainly be explained by the EDA interactions. Stronger EDA
266 interaction might be possible when the π -electron depletes any aromatic ring and π -electron rich
267 regions interacts together (Ahmed et al., 2017b). Antibiotics such as SMT, STZ and SMX can act
268 as π -electron-acceptor due to their amino functional groups (donating lone pair electrons to the
269 arene unit) and N and/or O-hetero-aromatic rings (electronic resonance). While CP can also act as
270 π -electron-acceptor site due to its nitro group presence on its arene unit. Moreover, fBC enriched
271 with C=C and C \equiv C groups along with -OH, C=O and -COOH groups and may act as a strong π -
272 electron-donor or acceptor sites at pH ~ 1.5 . The pK_a values of surface -COOH and surface -OH
273 are ~ 3.0 - 5.0 and above 8.0 , respectively, hence proton exchange is not possible for those
274 functional groups (Teixidó et al., 2011). However, hydroxyl group in fBC can acts as π -electron
275 donor due to its π -electron donor capacity to the arene unit in fBC, while surface -COOH and -

276 C=O may act as opposite effect due to its π -electron withdrawal capacity from the arene unit.
 277 Hence, at low pH, EDA interactions between –OH groups in fBC and π -electron depleted
 278 aromatic unit in antibiotics might be the main sorption mechanism (**Fig. 4**). The π - π electron-
 279 acceptor-acceptor (EAA) interactions (due to BC-C=O group and BC-COOH group become
 280 electron acceptor as well as antibiotics molecules can behave as electron acceptor site) might also
 281 possible but not stronger than EDA interactions (**Fig. 4**). So, at very low pH, competitive sorption
 282 of sulfonamides and CP antibiotics on to positively charged fBC were mainly due to EDA
 283 interactions and this result is also supported by previous study (Ahmed et al., 2017b; Teixidó et
 284 al., 2011).

285 At pH ~4.0, all sulfonamide antibiotics behaved as neutral species in the solution and CP
 286 was more stable. Maximum sorption of all selected antibiotics in competitive mode was found at
 287 this pH range. In addition to EDA, strong hydrogen bonds and CAHB formations might be the
 288 main sorption mechanisms. As mentioned earlier, the pK_a value of surface –COOH was near
 289 ~3.0-5.0, hence, hydrogen bond formations were highly possible among fBC surface –COOH
 290 groups and with –NH₂ or, –NO₂ or hydrogen groups present in sulfonamides and CP antibiotics.



295 Proton exchange with water molecule should increase the solution pH by leaving –OH groups in
 296 the solution and thus final solution pH should be increased. However, pH shifted to become more
 297 acidic indicating that **equation 7** was not the main mechanism (**Fig. 2**), which is consistent with
 298 previous studies (Ahmed et al., 2017b, Teixidó et al., 2011). This might be due to the formation
 299 of strong H-bond formations for neutral sulfonamides (**equation 8**). The **equation 9** involves

300 tautomerisation of sulfonamides to the zwitterion in the adsorbed state while **equation 10** shows
 301 the tautomerisation by forming the zwitterion and releasing protons in the solution. Thus, the
 302 observed equilibrium pH slightly decreased from the initial pH and stabilization of **equations 9**
 303 **and 10** might be possible through the formation of a π - π EDA which might not be as strong as
 304 the positively charged sulfonamide ring system with the biochar surface. Overall stabilization of
 305 the cationic form of sulfonamides can be gained through a strong H-bond formation (**Fig. 4**).

306 On the other hand, CP has a pK_a value of ~ 5.50 and thus ΔpK_a for surface $-\text{COOH}$ and
 307 CP lays ~ 1.0 - 1.5 . Normally, smaller the difference stronger the hydrogen bond formations (Gilli
 308 et al., 2008). More clearly, CP can initially undergo for proton exchange with water molecule and
 309 release of $-\text{OH}$ in solution (**equation 11**) and the $-\text{OH}$ may be neutralize by releasing proton
 310 from surface $-\text{COOH}$ to form negative CAHB (**equation 12**). This was resulted in slightly
 311 decrease in equilibrium pH (**Fig. 2**). Thus at pH ~ 4.0 - 4.25 , sulfonamides antibiotics molecules
 312 mainly formed strong hydrogen bonds whereas CP formed CAHB along with EDA interactions,
 313 which were the main reasons for higher sorption of those antibiotics. Moreover, ordinary
 314 hydrogen bonds formation among hydrogen in CP and $-\text{COOH}$ in fBC might also responsible for
 315 the high affinity. The π - π EAA interaction was less effective as biochar surface became negative
 316 above pH 2.2 and as surface carboxylate group had pK_a values more than 4.



319 Lewis acid base electronic interaction might be possible at pH of ~ 4.0 where sulfonamides
 320 remain as a neutral species and thus, loan-pair electrons of amino groups in the arene unit may
 321 donate to form a complex with the protonated enriched surface functional groups (Ahmed et al.,
 322 2017b).

323 At pH near 5.5, all the sulfonamide antibiotics remained as minimum ionized states due to
 324 intersections points and thus minimum sorption at this pH was found. At the same time,
 325 minimum CP sorption was also found (might be just crossing the pK_a matched solution pH).
 326 Equilibrium pH moved to ~6.4 also indicating the release of –OH groups in the solution by
 327 consuming proton from the solution leading to hydrogen bond formations.

328 In alkaline solution, the sorption of sulfonamide negative species was found to be
 329 significantly lower than for neutral species. This was due to repulsion of negative species
 330 sulfonamides as well as negative surface fBC. Teixidó et al. (2011) noted that the adsorption of
 331 SMT^- was due to the release of –OH for proton exchange with water molecule ($SMT^- + H_2O \rightarrow$
 332 $SMT^0 + OH^-$), followed by interactions of the resulting natural molecules with surface –COOH
 333 and –OH groups ($SMT^0 + BC = SMT^0 \dots BC$). These kinds of bonds formation were designed as
 334 strong negative CAHB. They mentioned that pH was raised as SMT^- sorption amount increased.
 335 However, in this study it was found equilibrium pH was decreased indicating that protons were
 336 released by fBC surface. As the pK_{a2} values of all sulfonamides ranged from 6.16 to 6.99 and pK_a
 337 values of phenolic groups ranged from 7 to 10 (Gilli et al., 2008), ΔpK_a value between phenolic
 338 groups and sulfonamide groups is around ~0.0-2.5. Thus, initially, sulfonamide antibiotics began
 339 with proton exchange with water molecules hence releasing –OH in solution (**equation 13**),
 340 followed by neutralization of hydroxyl groups by the release of protons from fBC surface –OH
 341 groups through the formation of negative CAHB (**equation 14**).



344 CP might form CAHB and weak hydrogen bonds among surface hydroxyl groups of fBC,
 345 aromatic nitro group and hydroxyl groups (**Fig. 4**). EDA interactions for CP were not favorable at

346 this pH since the hydroxyl group was deprotonated to form CAHB. In addition, EAA could be
347 possible due to unchanged $-\text{COOH}$ groups on fBC surface.

348

349 *3.5. Treatment of water and synthetic wastewater during competitive removal*

350 Competitive removal of antibiotics was carried out at different dosages of fBC and pronounced
351 differences were observed for lake and synthetic wastewater (**Fig. 5**). In comparison with lake
352 water, synthetic wastewater was found to have more influence on antibiotics removal than lake
353 water. Final lake water TOC value was found to be 46.53 mg L^{-1} . The synthetic wastewater
354 contained different chemicals in the form of inorganic and organic species that could compete
355 with the antibiotics for fBC sorption sites and resulted in lower sorption efficiency with final
356 TOC value of 50.5 mg L^{-1} . Regarding antibiotics themselves, in both water types, STZ sorbed
357 even at 200 mg L^{-1} dosage of fBC while SMT required a higher dosage ($\sim 700 \text{ mg L}^{-1}$ of fBC,
358 synthetic wastewater) for the complete removal from the mixture solution. Overall, the trend for
359 removing selected antibiotics in competitive mode followed the order of deionized water > lake
360 surface water > synthetic wastewater. Therefore, fBC could be successfully applied for the
361 treatment of a mixture of antibiotics from different water and wastewater.

362

363 **4. Conclusions**

364 Competitive sorption of sulphonamides and chloramphenicol was very strong toward fBC.
365 Competitive sorption was governed by solution pH and the maximum sorption occurred at pH
366 4.0-4.25. Sorption affinity decreased in the order $\text{STZ} < \text{SMX} < \text{CP} < \text{SMT}$. fBC was found to be
367 highly efficient in removing these antibiotics from water and wastewater, with the sorption
368 affinity following the order of deionized water > lake water > synthetic wastewater. The sorptive
369 mechanisms were addressed in detail based on resonance effect of arene units. The results

370 demonstrate that fBC is very effective in removing antibiotics mixture from water and
371 wastewater.

372

373 **5. Supplementary information**

374 Physicochemical properties of the antibiotics (Table A1), summary of the kinetic model
375 parameters for antibiotics sorption on fBC (Table A2), EDS data for fBC (Table A3), FTIR and
376 Raman spectra of fBC before and after sorption (Fig. A1), possible resonance structures of
377 antibiotics and fBC and their electron donor and acceptor sites (Fig. A2).

378

379 **6. Acknowledgements**

380 The authors thank the Faculty of Engineering and Information Technology, University of
381 Technology Sydney for providing Faculty and IRS scholarships. Special thanks to New Forest
382 Asset Management Pty Ltd, Victoria, Australia for providing *Eucalyptus Globulus* wood
383 samples.

384

385 **References**

- 386 1. Ahmed M.B., Zhou J.L., Ngo H.H., Guo W.S., 2015. Adsorptive removal of antibiotics from
387 water and wastewater: Progress and challenges. *Sci. Total Environ.* 532, 112-126.
- 388 2. Ahmed M.B., Zhou J.L., Ngo H.H., Guo W.S., Chen M., 2016a. Progress in the preparation
389 and application of modified biochar for improved contaminant removal from water and
390 wastewater. *Bioresour. Technol.* 214, 836-851.
- 391 3. Ahmed M.B., Zhou J.L., Ngo H.H., Guo W.S., 2016b. Insight into biochar properties and its
392 cost analysis. *Biomass Bioenerg.* 84, 76-86.

- 393 4. Ahmed M.B., Zhou J.L., Ngo H.H., Guo W.S., Thomaidis N.S., Xu J., 2017a. Progress in the
394 biological and chemical treatment technologies for emerging contaminant removal from
395 wastewater: A critical review. *J. Hazard. Mater.* 323, 274-298.
- 396 5. Ahmed M.B., Zhou J.L., Ngo H.H., Guo W.S., Johir M.A.H., Sornalingam K., 2017b. Single
397 and competitive sorption properties and mechanism of functionalized biochar for removing
398 sulfonamide antibiotics from water. *Chem. Eng. J.* 311, 348-358.
- 399 6. Azhar M.R., Abid H.R., Sun H., Periasamy V., Tadé M.O., Wang S., 2016. Excellent
400 performance of copper based metal organic framework in adsorptive removal of toxic
401 sulfonamide antibiotics from wastewater. *J. Colloid Interface Sci.* 478, 344-352.
- 402 7. Carvalho I.T. and Santos L., 2016. Antibiotics in the aquatic environments: a review of the
403 European scenario. *Environ. In.* 94, 736-757.
- 404 8. Calisto V., Jaria G., Silva C.P., Ferreira C.I., Otero M., Esteves V.I., 2017. Single and multi-
405 component adsorption of psychiatric pharmaceuticals onto alternative and commercial
406 carbons. *J. Environ. Manag.* 192, 15-24.
- 407 9. Chen, D., Yu, X., Song, C., Pang, X., Huang, J., Li, Y., 2016. Effect of pyrolysis temperature
408 on the chemical oxidation stability of bamboo biochar. *Bioresour. Technol.* 218, 1303-1306.
- 409 10. Cui, E., Wu, Y., Zuo, Y., Chen, H. 2016. Effect of different biochars on antibiotic resistance
410 genes and bacterial community during chicken manure composting. *Bioresour. Technol.* 203,
411 11-17.
- 412 11. Devi, P., Saroha, A.K., 2014. Synthesis of the magnetic biochar composites for use as an
413 adsorbent for the removal of pentachlorophenol from the effluent. *Bioresour. Technol.* 169,
414 525-531.
- 415 12. Fukahori, S., Fujiwara, T., Ito, R., Funamizu, N., 2011. pH-dependent adsorption of sulfa
416 drugs on high silica zeolite: modeling and kinetic study. *Desalination* 275, 237-242.

- 417 13. Gilli P., Pretto L., Bertolasi V., Gilli G., 2008. Predicting Hydrogen-Bond Strengths from
418 Acid– Base Molecular Properties. The pKa Slide Rule: Toward the Solution of a Long-
419 Lasting Problem. *Acc. Chem. Res.* 42, 33-44.
- 420 14. Grover D., Zhou, J.L., Frickers, P.E., Readman, J.W., 2011. Improved removal of estrogenic
421 and pharmaceutical compounds in sewage effluent by full scale granular activated carbon:
422 impact on receiving river water. *J. Hazard. Mater.* 185, 1005-1011.
- 423 15. Lian F., Sun B., Song Z., Zhu L., Qi X., Xing B., 2014. Physicochemical properties of herb-
424 residue biochar and its sorption to ionizable antibiotic sulfamethoxazole. *Chem. Eng. J.* 248,
425 128-134.
- 426 16. Nielsen L. and Bandosz T.J., 2016. Analysis of the competitive adsorption of pharmaceuticals
427 on waste derived materials. *Chem. Eng. J.* 287, 139-147.
- 428 17. Maskaoui K. and Zhou J.L., 2010. Colloids as a sink for certain pharmaceutical in the aquatic
429 environment. *Environ. Sci. Pollut. Res.* 17, 898-907.
- 430 18. Pavlović D.M., Ćurković L., Blažek D., Župan J., 2014. The sorption of sulfamethazine on
431 soil samples: Isotherms and error analysis. *Sci. Total Environ.* 497, 543-552.
- 432 10. Pei, Z., Yang, S., Li, L., Li, C., Zhang, S., Shan, X. Q., Wen, B., Guo, B., 2014. Effects of
433 copper and aluminum on the adsorption of sulfathiazole and tylosin on peat and soil.
434 *Environ. Pollut.* 184, 579-585.
- 435 20. Rajapaksha, A.U., Vithanage, M., Zhang, M., Ahmad, M., Mohan, D., Chang, S.X., Ok, Y.S.,
436 2014. Pyrolysis condition affected sulfamethazine sorption by tea waste biochars. *Bioresour.*
437 *Technol.* 166, 303–308.
- 438 21. Seifrtová M., Nováková L., Lino C., Pena A., Solich P., 2009. An overview of analytical
439 methodologies for the determination of antibiotics in environmental waters. *Anal. Chim.*
440 *Acta* 649, 158-179.

- 441 22. Tang, J., Lv, H., Gong, Y., Huang, Y., 2015. Preparation and characterization of a novel
442 graphene/biochar composite for aqueous phenanthrene and mercury removal. *Bioresour.*
443 *Technol.* 196, 355–363
- 444 23. Teixidó M., Pignatello J.J., Beltrán J.L., Granados M., Peccia J., 2011. Speciation of the
445 ionizable antibiotic sulfamethazine on black carbon (biochar). *Environ. Sci. Technol.* 45,
446 10020-10027.
- 447 24. Veksha, A., McLaughlin, H., Layzell, D. B., Hill, J. M., 2014. Pyrolysis of wood to biochar:
448 Increasing yield while maintaining microporosity. *Bioresour. Technol.* 153, 173-179.
- 449 25. Wang, B., Jiang, Y. S., Li, F. Y., Yang, D. Y. 2017. Preparation of biochar by simultaneous
450 carbonization, magnetization and activation for norfloxacin removal in water. *Bioresour.*
451 *Technol.* 233, 159-165.
- 452 26. Wang, F., Ren, X., Sun, H., Ma, L., Zhu, H., Xu, J., 2016. Sorption of polychlorinated
453 biphenyls onto biochars derived from corn straw and the effect of propranolol. *Bioresour.*
454 *Technol.* 219, 458-465.
- 455 27. Xie A., Dai J., Chen X., Zou T., He J., Chang Z., Li C., Yan Y., 2016. Hollow imprinted
456 polymer nanorods with a tunable shell using halloysite nanotubes as a sacrificial template for
457 selective recognition and separation of chloramphenicol. *RSC Adv.* 6, 51014-51023
- 458 28. Xie M., Chen W., Xu Z., Zheng S., Zhu D., 2014. Adsorption of sulfonamides to
459 demineralized pine wood biochars prepared under different thermochemical conditions.
460 *Environ. Pollut.* 186, 187-194.
- 461 29. Yao Y., Gao B., Chen H., Jiang L., Inyang M., Zimmerman A.R., Cao X., Yang L., Xue Y.,
462 Li H., 2012. Adsorption of sulfamethoxazole on biochar and its impact on reclaimed water
463 irrigation. *J. Hazard. Mater.* 209, 408-413.

- 464 30. Yu F., Li Y., Han S., Ma J., 2016. Adsorptive removal of antibiotics from aqueous solution
465 using carbon materials. *Chemosphere* 153, 365-385.
- 466 31. Zhao H., Liu X., Cao Z., Zhan Y., Shi X., Yang Y, Zhou J., Xu J., 2016. Adsorption
467 behavior and mechanism of chloramphenicols, sulfonamides, and non-antibiotic
468 pharmaceuticals on multi-walled carbon nanotubes. *J. Hazard. Mater.* 310, 235-245.
- 469 32. Zheng H., Wang Z., Zhao J., Herbert S., Xing B., 2013. Sorption of antibiotic
470 sulfamethoxazole varies with biochars produced at different temperatures. *Environ. Pollut.*
471 181, 60-67.

472 **Figure captions**

473

474 **Fig. 1.** Effect of pH on K_d (with standard deviation) during the removal of sulfonamides and
475 chloramphenicol antibiotics using fBC (80 mg L⁻¹) with initial individual antibiotic concentration
476 of 1.0 mg L⁻¹ at 25 °C (a). Competitive sorption kinetics data with PSO and PFO model fitting
477 using 1.0 mg L⁻¹ initial antibiotics concentration and 80 mg L⁻¹ of fBC at pH 4.0- 4.25 (b).

478

479 **Fig. 2.** Zeta potential values of fBC and pH shift during pH effect study.

480

481 **Fig. 3.** Sorption isotherm plots and model fitting for mixtures of antibiotics (initial concentration
482 of each antibiotic was 0.250-20.0 mg L⁻¹) at pH 4.0-4.25 using fBC dosage of 80 mg L⁻¹.

483

484 **Fig. 4.** Proposed sorption mechanisms for the removal of antibiotics in competitive mode using
485 fBC.

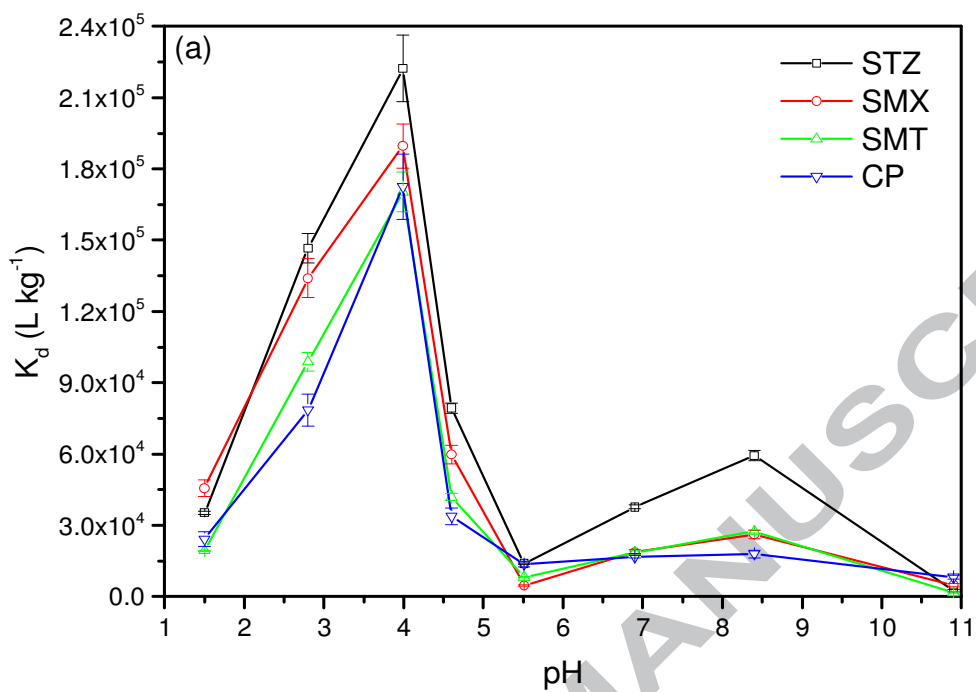
486

487 **Fig. 5.** Sorption of antibiotics (%) in mixture mode with 1.0 mg L⁻¹ initial concentration of each
488 antibiotic from lake water (a) and synthetic wastewater (b) with different dosages of fBC at pH
489 4.0-4.25 and 25 °C.

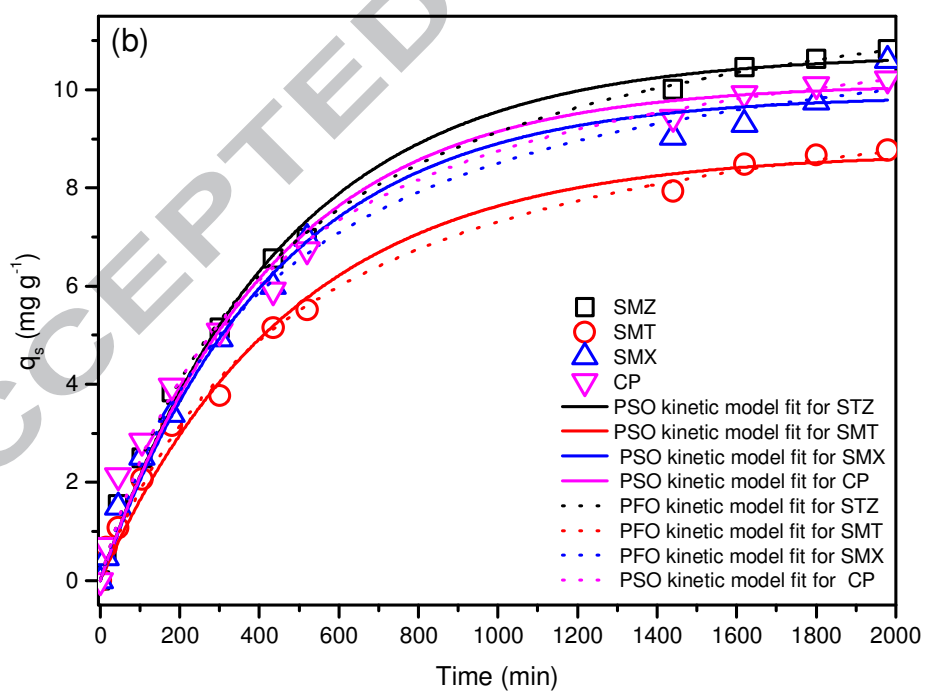
490

491

Fig. 1.



492

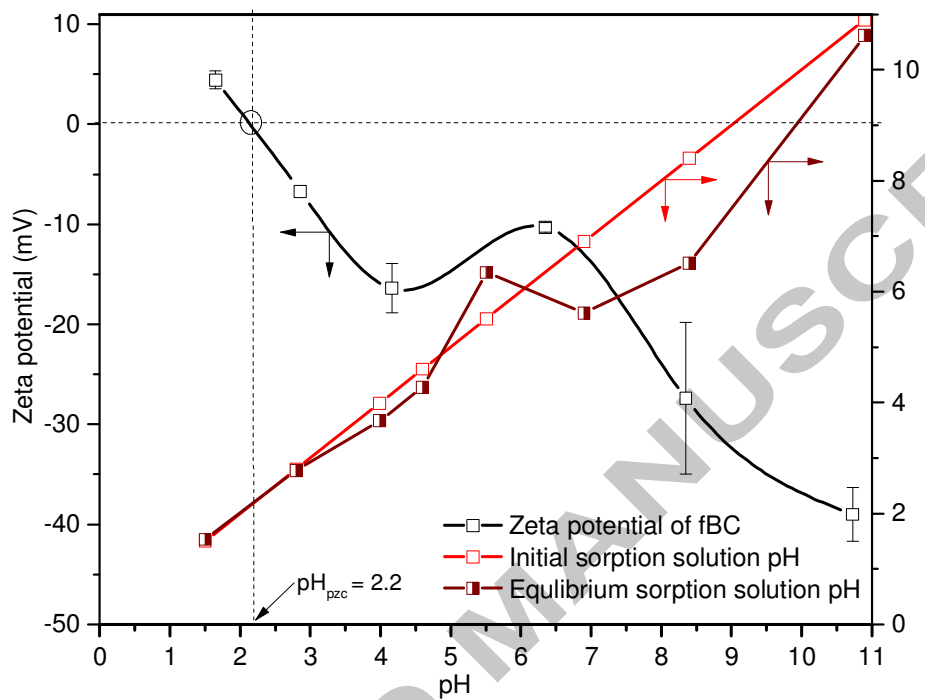


493

494

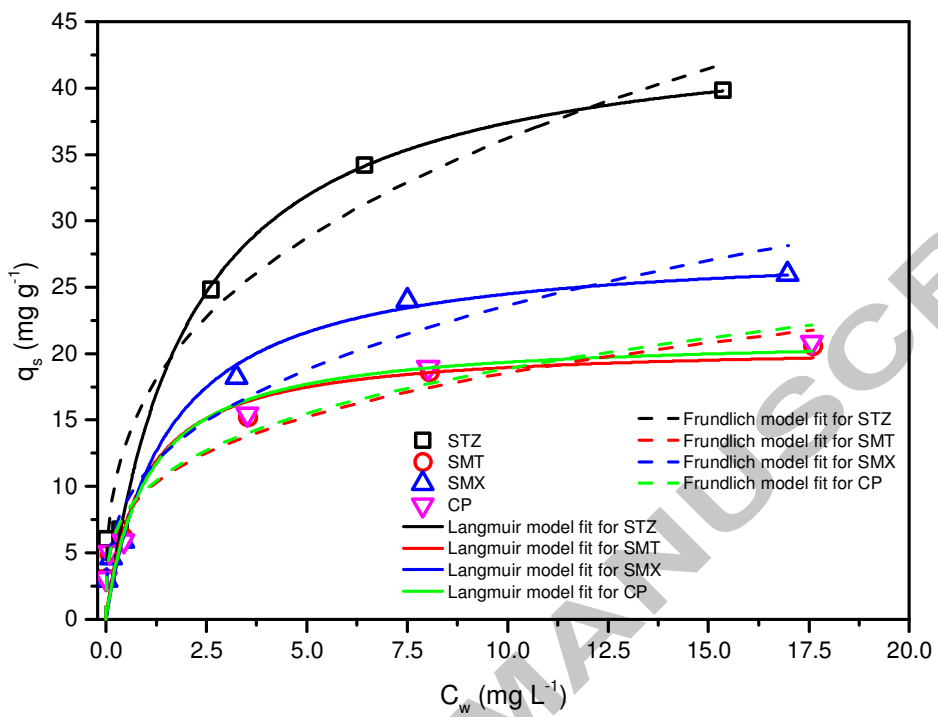
495

Fig. 2.

496
497

498
499

Fig. 3.



500

501
502
503
504

Fig. 4.

Competitive Sorption Affinity Mechanisms

At very low pH:

- (i). Repulsion interactions
- (ii). BC-OH + sulfonamides/CP = EDA interactions

At pH 4.0-4.25:

- (i). BC-COO⁻.....H⁺.....⁻O₂N-chloramphenicol = CAHB formations with EDA interactions
- (ii). BC-COO⁻.H + sulfonamides (NHSO₂⁻/NH⁻/-NH₂/CH₃) = H-bond formations

At pH above 7.0:

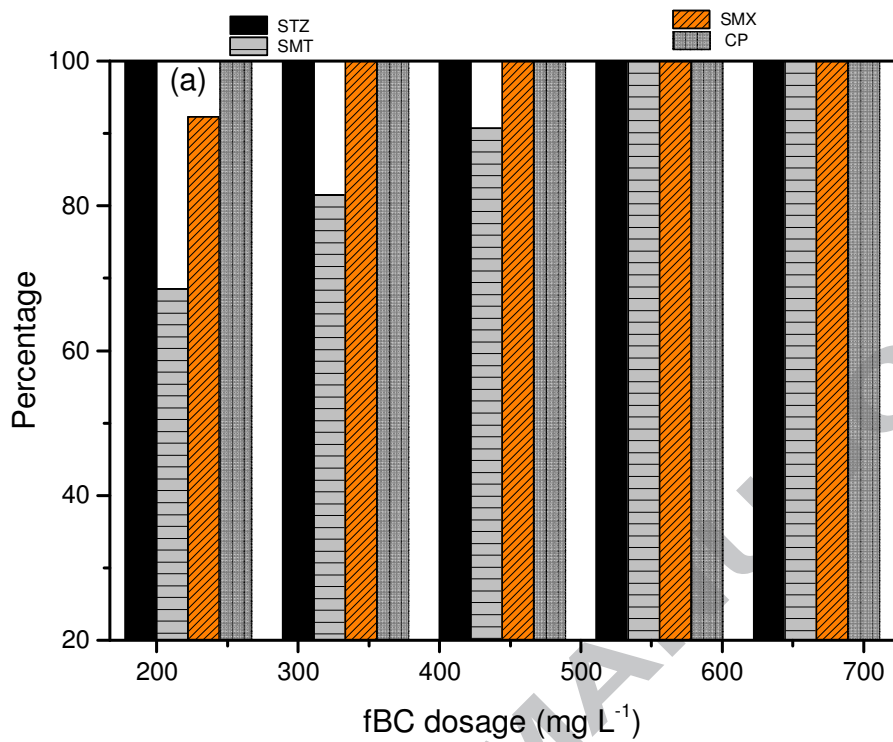
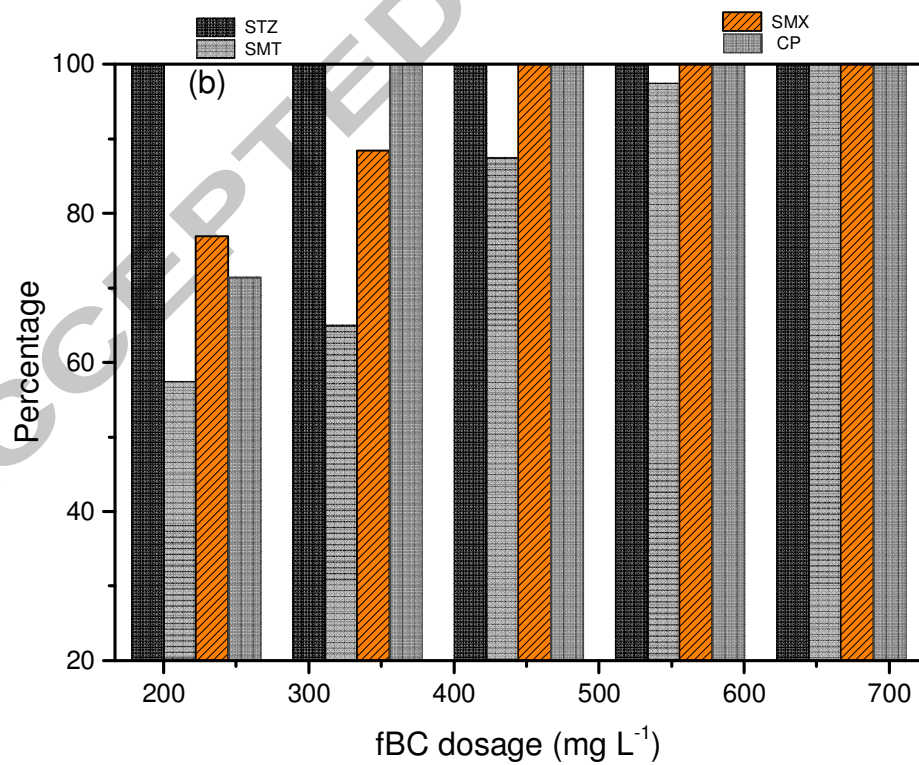
- (i). Repulsion interactions
- (ii). Sulfonamides-N⁺ + H₂O = sulfonamides-NH + -OH⁺
- (iii). BC-O⁻....H + N⁺....sulfonamides = BC-O⁻.....H⁺.....N⁺....sulfonamides = CAHB
- (iv). BC-OH + chloramphenicol (H⁺/-OH/NO₂⁻/-NH⁻/-Cl) = H-bond formations

505
506

ACCEPTED MANUSCRIPT

507
508

Fig. 5.

509
510511
512

513 **Table 1.** Summary of the Freundlich and Langmuir isotherm parameters for competitive
 514 antibiotic sorption on fBC at 25 ± 0.5 °C.

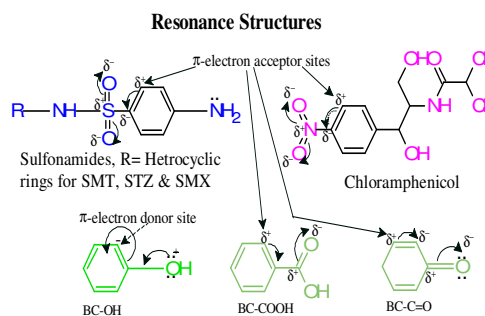
Antibiotic	Freundlich isotherm parameters			Langmuir isotherm parameters		
	K_F	n	R^2	q_{max}	K_L	R^2
STZ	16.76±2.53	2.99±0.60	0.942	45.19±5.03	0.48±0.20	0.956
SMT	9.65±1.21	3.52±0.67	0.930	20.71±1.99	1.08±0.54	0.915
SMX	11.04±1.33	3.03±0.47	0.949	28.29±2.30	0.65±0.23	0.965
CP	9.81±1.28	3.52±0.70	0.925	21.35±2.27	0.97±0.52	0.906

515

516

517

518 Graphical abstract

**Sorption Affinity Mechanisms**

Competitive Sorption Affinity: STZ> SMX> CP>SMT

At very low pH:

- (i). Repulsion interactions
- (ii). BC-OH + sulfonamides/CP = EDA interactions

At pH 4.0-4.25:

- (i). BC-COO⁻...H⁺...O₂N-chloramphenicol = CAHB formations with EDA interactions
- (ii). BC-COO⁻.H + sulfonamides (NHSO₂/NH/-NH₂/CH₃) = H-bond formations

At pH above 7.0:

- (i). Repulsion interactions
- (ii). Sulfonamides-N⁻ + H₂O = sulfonamides-NH + -OH⁺
- (iii). BC-O⁻...H + N...sulfonamides = BC-O⁻...H⁺...N...sulfonamides = CAHB
- (iv). BC-OH + chloramphenicol (H⁺/OH/NO₂/-NH/-Cl) = H-bond formations

Comparative Treatment Trend:

Deionized water> Lake water > Synthetic wastewater

519

520

521

522

523 **Highlights**

524

525 ❖ Competitive sorption affinities followed the order: STZ > SMX > CP > SMT.

526 ❖ Maximum sorption affinity was found at pH ~4.0-4.25 for all antibiotics.

527 ❖ Main sorption mechanisms were H-bonds and charge assisted hydrogen bond formation.

528 ❖ Electron-donor-acceptor interactions also played a significant role.

529 ❖ Sorption decreased as deionized water > lake water > synthetic wastewater.

530

ACCEPTED MANUSCRIPT